SINTEF
PROCEEDINGS
2

Proceedings of the 12th International Conference on Computational Fluid Dynamics in the Oil & Gas, Metallurgical and Process Industries

Progress in Applied CFD – CFD2017

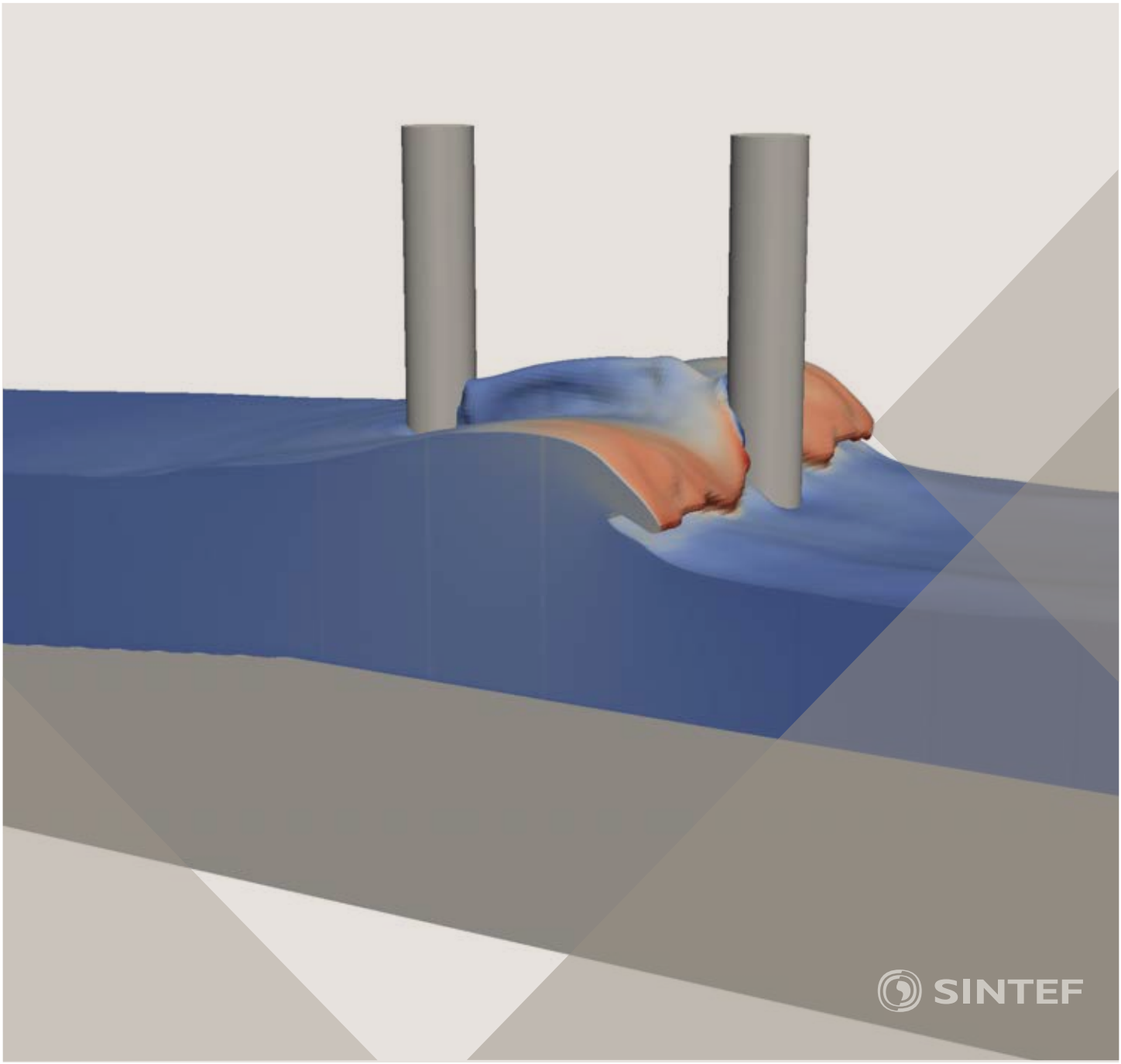

SINTEF Proceedings

Editors:
Jan Erik Olsen and Stein Tore Johansen

Progress in Applied CFD – CFD2017

Proceedings of the 12th International Conference on Computational Fluid Dynamics in the Oil & Gas, Metallurgical and Process Industries

SINTEF Academic Press

SINTEF Proceedings no 2
Editors: Jan Erik Olsen and Stein Tore Johansen
Progress in Applied CFD – CFD2017
Selected papers from 10th International Conference on Computational Fluid Dynamics in the Oil & Gas, Metallurgical and Process Industries

Key words:
CFD, Flow, Modelling

Cover, illustration: Arun Kamath

ISSN 2387-4295 (online)
ISBN 978-82-536-1544-8 (pdf)

© Copyright SINTEF Academic Press 2017
The material in this publication is covered by the provisions of the Norwegian Copyright Act. Without any special agreement with SINTEF Academic Press, any copying and making available of the material is only allowed to the extent that this is permitted by law or allowed through an agreement with Kopinor, the Reproduction Rights Organisation for Norway. Any use contrary to legislation or an agreement may lead to a liability for damages and confiscation, and may be punished by fines or imprisonment

SINTEF Academic Press
Address: Forskningsveien 3 B
PO Box 124 Blindern
N-0314 OSLO
Tel: +47 73 59 30 00
Fax: +47 22 96 55 08

www.sintef.no/byggforsk
www.sintefbok.no

SINTEF Proceedings
SINTEF Proceedings is a serial publication for peer-reviewed conference proceedings on a variety of scientific topics.
The processes of peer-reviewing of papers published in SINTEF Proceedings are administered by the conference organizers and proceedings editors. Detailed procedures will vary according to custom and practice in each scientific community.

PREFACE

This book contains all manuscripts approved by the reviewers and the organizing committee of the 12th International Conference on Computational Fluid Dynamics in the Oil & Gas, Metallurgical and Process Industries. The conference was hosted by SINTEF in Trondheim in May/June 2017 and is also known as CFD2017 for short. The conference series was initiated by CSIRO and Phil Schwarz in 1997. So far the conference has been alternating between CSIRO in Melbourne and SINTEF in Trondheim. The conferences focuses on the application of CFD in the oil and gas industries, metal production, mineral processing, power generation, chemicals and other process industries. In addition pragmatic modelling concepts and bio-mechanical applications have become an important part of the conference. The papers in this book demonstrate the current progress in applied CFD.

The conference papers undergo a review process involving two experts. Only papers accepted by the reviewers are included in the proceedings. 108 contributions were presented at the conference together with six keynote presentations. A majority of these contributions are presented by their manuscript in this collection (a few were granted to present without an accompanying manuscript).

The organizing committee would like to thank everyone who has helped with review of manuscripts, all those who helped to promote the conference and all authors who have submitted scientific contributions. We are also grateful for the support from the conference sponsors: ANSYS, SFI Metal Production and NanoSim.

Stein Tore Johansen & Jan Erik Olsen

Organizing committee:

Conference chairman: Prof. Stein Tore Johansen
Conference coordinator: Dr. Jan Erik Olsen
Dr. Bernhard Müller
Dr.Sigrid Karstad Dahl
Dr.Shahriar Amini
Dr.Ernst Meese
Dr.Josip Zoric
Dr.Jannike Solsvik
Dr.Peter Witt

Scientific committee:

Stein Tore Johansen, SINTEF/NTNU
Bernhard Müller, NTNU
Phil Schwarz, CSIRO
Akio Tomiyama, Kobe University
Hans Kuipers, Eindhoven University of Technology
Jinghai Li, Chinese Academy of Science
Markus Braun, Ansys
Simon Lo, CD-adapco
Patrick Segers, Universiteit Gent
Jiyuan Tu, RMIT
Jos Derksen, University of Aberdeen
Dmitry Eskin, Schlumberger-Doll Research
Pär Jönsson, KTH
Stefan Pirker, Johannes Kepler University
Josip Zoric, SINTEF

CONTENTS

COMBINED MULTIFLUID-POPULATION BALANCE METHOD FOR POLYDISPERSE MULTIPHASE FLOWS

Alexander VIKHANSKY

Siemens PLM Software, Trident House, Basil Hill Road, Didcot OX11 7HJ, UK

E-mail: alexander.vichansky@cd-adapco.com

ABSTRACT

In the present work we analyse applicability of the adaptive multiple size-group (A-MuSiG) population balance method to modelling of multiphase flows. The dispersed phase is split into M size-groups, each one having its own mass- and momentum balance. An additional equation for the number density makes the method adaptive, that is, the groups sizes are not prescribed a priory, but calculated. A special attention is paid to the effect of the turbulent diffusion on size distribution. The method is implemented in the multiphase CFD code STAR-CCM+ of Siemens PLM Software.

Keywords: CFD, population balance, two-phase flows .

NOMENCLATURE

Greek Symbols

α	Volume fraction.
ρ	Mass density, $[kg/m^3]$.
τ	Reynolds stress, $[Pa]$.

Latin Symbols

D_T	Coefficient of turbulent diffusion, $[m^2/s]$.
L	Particle size, $[m]$.
M	Number of size groups.
m_{ij}	Group-to-group mass flux, $[kg/m^3 s]$.
n	Number density, $[m^{-3}]$.
$\mathbf{u}$	Velocity, $[m/s]$.
P	Pressure, $[kg/ms^2]$.
S	Number density source, $[m^{-3}s^{-1}]$.
v	Volume of a particle, $[m^3]$.

Sub/superscripts

p	Particle.

INTRODUCTION

Population balance equations (PBE) are the general mathematical framework describing different physical, chemical, biological, and technological processes (Ramkrishna, 2000). They deal with bubbles, droplets, bacteria, molecules, etc. Hereafter we call them "particles". Main object of a population balance equation is number density n, e.g., the number of particles having size, density, velocity and temperature in the intervals $[L, L+dL]$, $[\rho, \rho+d\rho]$, $[\boldsymbol{u}, \boldsymbol{u}+d\boldsymbol{u}]$, $[T, T+dT]$, respectively, is

$$n(L, \rho, \boldsymbol{u}, T) \times dL \times d\rho \times du_x \times du_y \times du_z \times dT. \quad (1)$$

In the most general form the PBE reads:

$$\frac{\partial n}{\partial t} = B(n) - D(n), \quad (2)$$

where B and D are "birth" and "death" rates due to transport, coalescence, breakup, mass transfer, etc. If a particle is characterised by a single parameter, e.g., size, Eq. (2) for $n(L)$ is called *univariate* PBE, otherwise it is *multivariate* PBE.

Eq. (1) provides a very detailed description of the system, e.g., momentum is given by the integral

$$\int (\rho \boldsymbol{u} n) dL d\rho d\boldsymbol{u} dT. \quad (3)$$

Therefore, by solving the PBE one gains more information than from solution of a Navier-Stokes (NS) equation. It is clear, that being a "theory of everything", the PBE in form of Eq. (2) is prohibitively time-consuming and has very little practical value; it is why more restricted, more tractable formulations are sought.

As an example imagine an isothermal bubbly flow. Inertia of the bubbles is low and one can assume with high confidence that the gas-liquid slip velocity depends on the local flow conditions and the bubble size only; the multivariate number density (1) can be represented as

$$n(L, \boldsymbol{u}) \approx n(L) \delta(\boldsymbol{u} - \boldsymbol{U}(L)), \quad (4)$$

where $\boldsymbol{U}(L) = \langle \boldsymbol{u} | L \rangle$ is the conditional mean velocity.

Method of classes (Kumar and Ramkrishna, 1996; Bhole *et al.*, 2008), also known as multisize-group (MuSiG) method (Lo, 1996) splits the dispersed (gas) phase into M size-groups, that is

$$n(L, \boldsymbol{u}) \approx \sum_{i=1}^{M} n(L_i) \delta(\boldsymbol{u} - \boldsymbol{U}(L_i)). \quad (5)$$

From the modelling point of view each group is a separate phase in every aspect but the name; the groups move with their own velocities and exchange mass, momentum and energy with other groups and with the continuous phase (Lo, 1996). Note that the method of classes in form (5) occupies an intermediate position between the univariate and full multivariate PBEs, to be precise, it is a *multivariate method with a first-order univariate conditional moment closure* (Klimenko and Bilger, 1999).

Recently, an adaptive discretisation has been proposed for the method of classes (Vikhansky, 2013; Vikhansky and Splawski, 2015), that is, the size-groups are not prescribed a priory, but follow the evolution of the size distribution. The first (simplified) version of the new adaptive multiple size-group method (A-MuSiG) has been implemented in a development version of the STAR-CCM+ simulation software of

Siemens PLM Software. The final version, described in the present paper, deals with the full set of the transport equations including turbulent dispersion and correct treatment of spurious dissipation.

MULTIFLUID MODEL

Reynolds-averaged (RA) mass conservation equation for the i^{th} group reads:

$$\frac{\partial \rho_p \overline{\alpha}_i}{\partial t} + \nabla \cdot (\rho_p \overline{\alpha}_i \langle \boldsymbol{u}_i \rangle_i) = m_{ij} - m_{ji}, \tag{6}$$

where ρ_p is density of the dispersed phase, $\overline{\alpha}_i$ is RA volume fraction of the i^{th} group and m_{ij}, m_{ji} are (averaged) mass fluxes from the j^{th} group to the i^{th} group and from the i^{th} group to the j^{th} group, respectively; $\langle \boldsymbol{u}_i \rangle_i$ is *phase-averaged* velocity of the group (Fox, 2014):

$$\langle \boldsymbol{u}_k \rangle_l = \frac{\langle \alpha_l \boldsymbol{u}_k \rangle}{\overline{\alpha}_l}, \tag{7}$$

where α_l, $\boldsymbol{u}_k$ are instantaneous values of volume fraction and velocity; angular brackets mean Reynolds averaging.
Reynolds-averaged momentum conservation equation for the i^{th} group reads:

$$\begin{aligned} \frac{\partial \rho_p \overline{\alpha}_i \langle \boldsymbol{u}_i \rangle_i}{\partial t} + \nabla \cdot (\rho_p \overline{\alpha}_i \langle \boldsymbol{u}_i \rangle_i \langle \boldsymbol{u}_i \rangle_i) = -\overline{\alpha}_i \nabla P \\ -\nabla \cdot \boldsymbol{\tau}_i + \langle \boldsymbol{F}_i \rangle + m_{ij} \langle \boldsymbol{u}_j \rangle_j - m_{ji} \langle \boldsymbol{u}_i \rangle_i, \end{aligned} \tag{8}$$

where $\boldsymbol{\tau}_i$ is Reynolds stress and $\boldsymbol{F}_i$ is interaction force between the continuous phase and the i^{th} group. The Reynolds stress $\boldsymbol{\tau}_i$ is modelled by a RANS model, which can be found elsewhere (Pope, 2000).
In order to calculate the phase interaction forces the size of the particles in the i^{th} group has to be specified. Prescribing a constant size for the group one obtains the MuSiG method (Lo, 1996). If the particles size distribution varies significantly across the system, the fixed discretisation in the size space is not efficient from the numerical point of view. In order to track the size distribution adaptively, Eqs. (6), (8) have to be augmented by an equation for the number density of the i^{th} group:

$$\frac{\partial \overline{n}_i}{\partial t} + \nabla \cdot \langle n_i \boldsymbol{u}_i \rangle = \langle S_i \rangle, \tag{9}$$

where S_i is the source term due to the breakage and coalescence of the particles, the RA number density flux is given below by Eq. (14). Knowing the number density one calculates the equivalent diameter of a particle as

$$d_i = \sqrt[3]{\frac{6\overline{\alpha}_i}{\pi \overline{n}_i}}. \tag{10}$$

In order to close the model described by Eqs. (6), (8), (9) one has to specify m_{ij} and $\langle S_i \rangle$; it is done by a population balance algorithm. Note that the population balance algorithm is local, that is, below we ignore the spatial variations of the parameters of interest and concentrate on a single cell of a finite volume method. Details of the A-MuSiG method are given in (Vikhansky, 2013; Vikhansky and Splawski, 2015). In a nutshell the method works as shown in Fig. 1; size of the circle on the diagram corresponds to the volume fraction of the size-group.

I Initially, all size-groups have the same volume fraction.

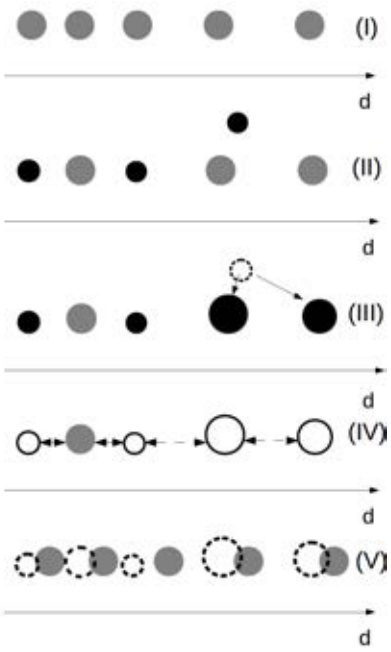

Figure 1: Schematic representation of the A-MuSiG method.

II When two size-groups undergo coalescence, a new particle is created, while the volume fraction and number densities of the parent size-groups reduces.

III Volume fraction and number density of the newly created particle is redistributed among two nearest size-groups using a version of the DQMoM method (Marchisio and Fox, 2005). At that step we locally conserve the first three moments of the distribution, namely, number density, mean volume (i.e., volume fraction), and mean square of the particles volume.

IV One can see that coalescence leads to depletion of the size-groups with small diameters and accumulation of the mass of the entire ensemble in the size-groups with higher diameters. In order to restore the equal distribution of the volume fractions, we redistribute the number density and volume fraction between each pair of neighbour groups. In each pair-wise redistribution event the first three moments of size distribution are conserved locally.

V By the end, each size-group has the same volume fraction, the size-groups have new diameters.

NUMBER DENSITY TRANSPORT

Note that it follows from Eq. (7) $\langle n_i \boldsymbol{u}_i \rangle \neq \overline{n}_i \langle \boldsymbol{u}_i \rangle_i$; in order to model the RA number density flux one can represent n_i as

$$n_i = \frac{\alpha_i}{v_i}. \tag{11}$$

Then

$$\langle n_i \boldsymbol{u}_i \rangle = \left\langle \alpha_i \boldsymbol{u}_i \frac{1}{v_i} \right\rangle = \overline{\alpha}_i \langle \boldsymbol{u}_i \rangle_i \frac{1}{\overline{v}_i} + \left\langle \alpha_i \boldsymbol{u}_i \left(\frac{1}{v_i} \right)' \right\rangle, \tag{12}$$

where the phase-averaged volume of a single particle is

$$\overline{v}_i = \frac{\overline{\alpha}_i}{\overline{n}_i}. \tag{13}$$

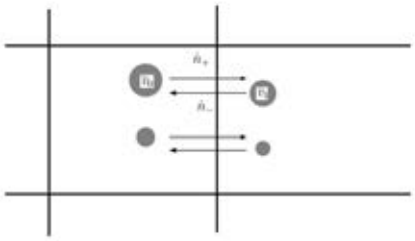

Figure 2: Schematic view of the diffusive flux.

Eq. (12) can be modelled using the gradient hypothesis:

$$\langle n_i \boldsymbol{u}_i \rangle = \overline{n}_i \langle \boldsymbol{u}_i \rangle_i - \overline{\alpha}_i D_T \boldsymbol{\nabla} \frac{1}{\overline{v}_i} = \overline{n}_i \left(\langle \boldsymbol{u}_i \rangle_i + D_T \boldsymbol{\nabla} \ln \overline{v}_i \right), \quad (14)$$

where D_T is coefficient of turbulent diffusion. There is no particular physical justification for (14) except that we use the same hypothesis for other scalars transported by turbulent flow field, e.g., kinetic energy of turbulence, temperature, etc. Note that if the group's volume $\overline{v}_i$ is constant, the diffusive flux in Eq. (14) vanishes.

The turbulence disperse the particles not just in the physical space, but also in the phase space. In order to illustrate this effect let as consider transport of the particles without breakup and coagulation. Since $\alpha_i = v_i n_i$ multiplication of the number density transport equation by v_i and subtraction from mass conservation after some algebra yields the equation for transport of the group's volume:

$$\frac{\partial v_i}{\partial t} + \boldsymbol{u}_i \cdot \boldsymbol{\nabla} v_i = 0. \quad (15)$$

It can be multiplied by v_i to result in

$$\frac{\partial v_i^2}{\partial t} + \boldsymbol{u}_i \cdot \boldsymbol{\nabla} v_i^2 = 0. \quad (16)$$

Eqs. (15)-(16) are averaged using the gradient closure:

$$\frac{\partial \langle v_i \rangle}{\partial t} + \langle \boldsymbol{u}_i \rangle \cdot \boldsymbol{\nabla} \langle v_i \rangle + \left\langle \boldsymbol{u}_i \cdot \boldsymbol{\nabla} v_i' \right\rangle = \frac{\partial \langle v_i \rangle}{\partial t} + \langle \boldsymbol{u}_i \rangle \cdot \boldsymbol{\nabla} \langle v_i \rangle - \boldsymbol{\nabla} \cdot \left(D_T \boldsymbol{\nabla} \langle v_i \rangle \right) = 0, \quad (17)$$

$$\frac{\partial \langle v_i^2 \rangle}{\partial t} + \langle \boldsymbol{u}_i \rangle \cdot \boldsymbol{\nabla} \langle v_i^2 \rangle + \left\langle \boldsymbol{u}_i \cdot \boldsymbol{\nabla} (v_i^2)' \right\rangle = \frac{\partial \langle v_i^2 \rangle}{\partial t} + \langle \boldsymbol{u}_i \rangle \cdot \boldsymbol{\nabla} \langle v_i^2 \rangle - \boldsymbol{\nabla} \cdot \left(D_T \boldsymbol{\nabla} \langle v_i^2 \rangle \right) = 0. \quad (18)$$

In order to obtain equation for the second central moment of the group's volume $\sigma_{v_i}^2 = \left\langle v_i^2 - \langle v_i \rangle^2 \right\rangle$ Eq. (17) is multiplied by $\langle v_i \rangle$ and subtracted from Eq. (18); after some algebra one obtains:

$$\frac{\partial \sigma_{v_i}^2}{\partial t} + \langle \boldsymbol{u}_i \rangle \cdot \boldsymbol{\nabla} \sigma_{v_i}^2 - \boldsymbol{\nabla} \cdot \left(D_T \boldsymbol{\nabla} \sigma_{v_i}^2 \right) = 2 D_T \left| \boldsymbol{\nabla} \langle v_i \rangle \right|^2. \quad (19)$$

Ignoring of the RHS in Eq. (19) leads to the spurious dissipation (underestimation of the standard deviation of the size distribution) obtained in (Marchisio and Fox, 2005; Fox, 2003).

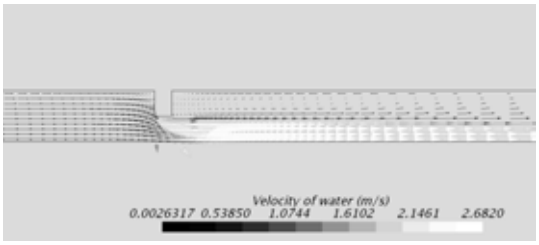

Figure 3: Water flow field.

Since the spurious dissipation is a result of the turbulent diffusion, proper discretisation of the diffusive flux might solve the problem (Vikas *et al.*, 2013). The root cause of the spurious dissipation can be illustrated by Fig. 2; the particles belonging to the same size-group at different neighbour cells have different diameters. It is not enough to calculate the total number density flux; one has to know the number $\dot{n}_+$ of the particles of size $\overline{v}_0$ moving from left to right, and number $\dot{n}_-$ of the particles of size $\overline{v}_1$ moving from right to left. Hereafter we use two conditions. Firstly, the difference between $\dot{n}_+$ and $\dot{n}_-$ is equal to the diffusive flux across the cell face:

$$\dot{n}_+ - \dot{n}_- = \overline{n}_f D_T \boldsymbol{\nu} \cdot \boldsymbol{\nabla} \ln \overline{v}, \quad (20)$$

where $\boldsymbol{\nu}$ is normal to the cell face and $\overline{n}_f$ is number density at the face. Secondly, the total mass flux by diffusion is zero, that is

$$\overline{v}_0 \dot{n}_+ = \overline{v}_1 \dot{n}_-. \quad (21)$$

Solution of Eqs. (20)-(21) yields:

$$\dot{n}_+ = \overline{n}_f \frac{\overline{v}_1}{\overline{v}_1 - \overline{v}_0} D_T \boldsymbol{\nu} \cdot \boldsymbol{\nabla} \ln \overline{v},$$
$$\dot{n}_- = \overline{n}_f \frac{\overline{v}_0}{\overline{v}_1 - \overline{v}_0} D_T \boldsymbol{\nu} \cdot \boldsymbol{\nabla} \ln \overline{v}. \quad (22)$$

Once the fluxes $\dot{n}_+$, $\dot{n}_-$ are calculated, corresponding numbers of particles with size $\overline{v}_0$, $\overline{v}_1$ are added to the right (left) cell according to the algorithm described in Fig. 1, (Vikhansky, 2013).

RESULTS AND DISCUSSION

Performance of the A-MuSiG method can be illustrated on a liquid-liquid pipe flow downstream of a restriction (Percy and Sleicher, 1983; Galinat *et al.*, 2005). The continuum phase is water, the dispersed phase is *n*-heptane. There is a recirculation zone behind the obstacle as shown in Fig. 3; the shear at the edge of the jet produces high dissipation rate, which causes intensive breakup of the droplets.

The adaptive nature of the method is demonstrated in Fig. 4; we perform the calculations with 5 size-groups and plot group diameters at the axis of the pipe. Initially, size of the biggest group increases because of coalescence, as the flow passes the orifice (at $x = 0$) a strong breakup happens. Fig. 4 can be interpreted in the following way: since there are 5 groups, one can say that approximately 10% of the droplets volume is below the first group diameter, 30% is below the second group diameter, etc., 90% is below the fifth group diameter. Since the A-MuSiG method is adaptive, only 5 size-groups suffice for quite detailed description of the size distribution.

For an M-independent characterisation of the droplets size distribution we use different definitions of mean diameters:

$$d_{pq} = \sqrt[p-q]{\frac{\sum n_i d_i^p}{\sum n_i d_i^q}}, \quad (23)$$

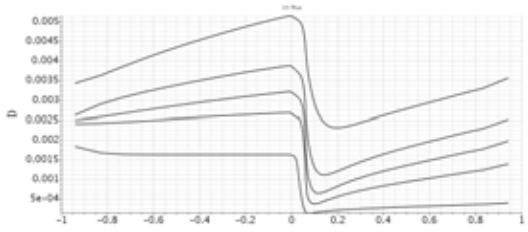

Figure 4: Group diameters at the pipe axis.

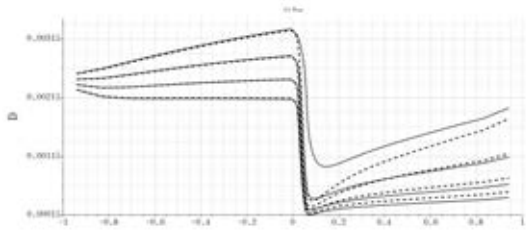

Figure 5: Mean diameters at the pipe axis with (dashed lines) and without (solid lines) spurious dissipation.

where the most important for applications are d_{43} (volume-mean diameter), d_{32} (Sauter mean diameter), d_{30} (volume-based diameter), and d_{10} (arithmetic mean diameter); $d_{43} \geq d_{32} \geq d_{30} \geq d_{10}$. For a mono-disperse system all diameters are equal; a high difference between, e.g., d_{43} and d_{10} implies a high standard deviation of the size distribution.

In order to examine the effect of the often-neglected spurious dissipation we plot all four mean diameters mentioned above in Fig. 5. As one could expect, the biggest error is just behind the obstacle where the size distribution undergoes the fastest change, and therefore the RHS in Eq. (19) is biggest. Calculations without a proper treatment of the spurious dissipation term significantly narrower size distribution than that using Eq. (22).

The M-dependence of the results is illustrated in Fig. 6. Apart from the fact that smaller M implies a narrower predicted distribution, one can see that $M = 3,\ 5,\ 9$ give quite close prediction of d_{43}, d_{32}, d_{30}, while calculation of d_{10} is less precise. It follows from the current formulation of the A-MuSiG method; since each size-group represents the same portion of volume fraction, more small particles are lumped together in the same (smallest) size-group. Even $M = 3$ resolves the distribution quite well up to $x \leq 0.2$, that is, breakup is less sensitive to the number of size-groups. For many applications the Sauter mean diameter d_{32} is the single most important particles size characteristics; our numerical experiments suggest that reliable engineering estimates can be done with a small ($M = 3 - 5$) number of the size-groups.

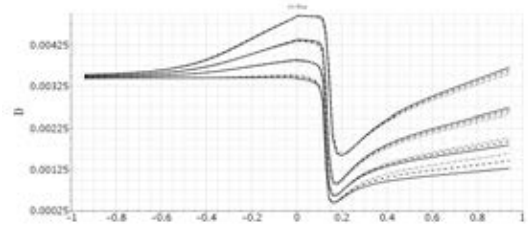

Figure 6: Mean diameters at the axis of the pipe calculated with 3 groups (dash-dotted), 5 groups (dotted), 9 groups (solid).

CONCLUSIONS

The paper presents an adaptive method for combined modelling of multiphase flows and breakup/coalescence processes; few size groups suffice for reliable prediction of mean characteristics of the polydisperse ensemble. The method solves for mass, momentum balance of each size-group, what extends it beyond a simple univariate population balance method. The effect of turbulent diffusion on size distribution is analysed and a special treatment is proposed to neutralize the spurious dissipation.

REFERENCES

BHOLE, M., JOSHI, J. and RAMKRISHNA, D. (2008). "CFD simulation of bubble columns incorporating population balance modeling". *Chemical Engineering Science*, **63**, 2267 – 2282.

FOX, R.O. (2003). *Computational models for turbulent reacting flows*. Cambridge University Press.

FOX, R.O. (2014). "On multiphase turbulence models for collisional fluid – particle flows". *JFM.*, **742**, 368 – 424.

GALINAT, S., MASBERNAT, O., GUIRAUD, P., DALMAZZONE, C. and NOÏK, C. (2005). "Drop break-up in turbulent pipe flow downstream of a restriction". *Chemical Engineering Science*, **60**, 6511 – 6528.

KLIMENKO, A. and BILGER, R. (1999). "Conditional moment closure for turbulent combustion". *Progress in Energy and Combustion Science*, **25**, 595 – 687.

KUMAR, S. and RAMKRISHNA, D. (1996). "On the solution of population balance equations by discretization - I. A fixed pivot technique". *Chem. Eng. Sci.*, **51**, 1311–1332.

LO, S. (1996). "Application of the MUSIG model to bubbly flows". *AEAT-1096, AEA Technology*, **230**, 8216–8246.

MARCHISIO, D.L. and FOX, R.O. (2005). "Solution of population balance equations using the direct quadrature method of moments". *J. Aerosol Sci.*, **36**, 43–73.

PERCY, J.S. and SLEICHER, C.A. (1983). "Drop breakup in the flow of immiscible liquids through an orifice in a pipe". *AIChE Journal*, **29**, 161–164.

POPE, S.B. (2000). *Turbulent Flows*. Cambridge University Press.

RAMKRISHNA, D. (2000). *Population balances*. Academic press.

VIKAS, V., WANG, Z. and FOX, R. (2013). "Realizable high-order finite-volume schemes for quadrature-based moment methods applied to diffusion population balance equations". *Journal of Computational Physics*, **249**, 162 – 179.

VIKHANSKY, A. (2013). "Direct quadrature spanning tree method for solution of the population balance equations". *Journal of Aerosol Science*, **55**, 78 – 88.

VIKHANSKY, A. and SPLAWSKI, A. (2015). "Adaptive multiple size group method for CFD-population balance modelling of polydisperse flows". *Canadian J. Chem. Eng.*